JOURNAL OF MATERIALS SCIENCE 31 (1996) 5199–5206

Evaluation of diffusion bonds formed between superplastic sheet materials

Z. C. WANG, N. RIDLEY, G. W. LORIMER
University of Manchester and UMIST, Materials Science Centre, Grosvenor Street, Manchester, M1 7HS, UK

D. KNAUSS, G. A. D. BRIGGS
Department of Materials, University of Oxford, Parks Road, Oxford, OX1 3PH, UK

Diffusion bonds produced in microduplex titanium and stainless steel sheet materials for various bonding conditions have been evaluated using a range of techniques. These include light and scanning electron microscopy (SEM), scanning acoustic microscopy (SAM) and compressive lap shear testing. The potential of other procedures such as ultrasonic inspection and resistivity measurement are also discussed. For imperfect bonds, the bond line in titanium alloys consists of clearly defined interfacial voids separated by metallurgically sound bonded regions, while the unbonded regions in stainless steel often consist of long flat voids in which the opposing surfaces have contacted but not bonded. It was observed that light microscopy and SEM observations provide a convenient and reliable method for the assessment of the bond quality, and in the case of titanium alloys it is possible to obtain quantitative data on the extent of bonding. High frequency SAM also proved to be an effective procedure for qualitative assessment. A linear relationship between the fraction of parent metal strength achieved and bonded area fraction as determined by metallography was observed for titanium alloys.

1. Introduction

Diffusion bonding (DB) is an important solid state process which can be used commercially to join similar and dissimilar materials. In theory, perfect bonds can be formed between two ideally atomically flat and clean surfaces by interatomic force without the application of an external pressure [1]. In practice, the surfaces to be bonded are not flat even at a macroscopic level, and are often contaminated, e.g. by the presence of oxide films. After cleaning, the two surfaces to be joined are brought into contact at an elevated temperature. Application of a moderate pressure brings the surfaces into intimate contact creating a planar array of interfacial voids. The subsequent removal of these interfacial voids is believed to be controlled by plastic deformation and diffusion processes [2–5]. For a given bonding temperature, the time to produce a sound bond with properties close or equal to that of the parent material depends on surface finish and applied bonding pressure. Assessment of bond quality is important because property data for the bonded region are required for quality control in DB practice.

A number of techniques have been developed for the evaluation of bond quality. These include metallography, ultrasonic inspection, and the use of mechanical testing procedures such as tensile, impact, and lap shear tests [6–8]. Mechanical testing may be combined with the use of scanning electron microscopy (SEM) to examine the fracture faces. Lap shear testing, using tensile or compressive loading, is the most convenient and most frequently used of the mechanical testing procedures for sheet materials. This method is useful for obtaining bond strength data and for quantitative evaluation of diffusion bonds. However, during shear testing, bending must be avoided without applying too large a constraining force.

Significant discrepancies can exist in the results obtained from different bond evaluation procedures [6, 7, 9–11]. For example, parent metal tensile strength has been reported for a mild steel when SEM examination of the fracture surface showed that bonding was only about 80% complete [10]. Impact strength and the area reduction observed after tensile testing have been reported to be reliable procedures for quantitative assessment of DB quality [6, 11]. However, these methods are not readily applicable to sheet materials. It is useful to investigate the techniques for the evaluation of diffusion bonds formed between sheet materials and to correlate the results obtained using various methods. In the present work, diffusion bonds produced in microduplex sheet materials using various bonding conditions were evaluated by metallographic techniques including light microscopy, scanning electron microscopy (SEM) scanning acoustic microscopy (SAM), and also by compressive lap

0022–2461

shear testing combined with SEM fractography. The relationship between the results obtained from metallographic methods and lap shear tests is examined.

2. Experimental procedure

Several advanced titanium alloys including IMI834 (Ti–5.8Al–4Sn–3.5Zr–0.7Nb–0.5Mo–0.3Si–0.05C), Ti–6Al–2Sn–4Zr–2Mo, SP700 (Ti–4.5Al–3V–2Fe–2Mo) and Super-Alpha-2 (Ti–14Al–19Nb–3V–2Mo) were used; compositions are in wt %. A commercial microduplex stainless steel was also examined. All materials were supplied in the form of sheet of thicknesses in the range of 0.5–3 mm and were isostatically bonded under various conditions. Three surface conditions were used: as-received (as-rolled), or ground using SiC paper to a P1200 or a P60 surface finish. In the latter cases, the grinding direction was parallel to the sheet rolling direction. The surfaces were cleaned in an ultrasonic bath containing methanol. The surface roughnesses as measured by a Talysurf (Talysurf 10, Rank Taylor Hobson Equipment) were $R_a = 0.2\ \mu m$ and $\lambda = 16\ \mu m$ for as-rolled sheet, $R_a = 0.1\ \mu m$ and $\lambda = 5\ \mu m$ for P1200 finish, and $R_a = 1.3\ \mu m$ and $\lambda = 7.5\ \mu m$ for P60 finish, where R_a is the arithmetic mean of the departure of the roughness profile from the mean line and λ is the wavelength. Pairs of rectangular blanks measuring 85 mm by 26 mm were electron beam welded around their peripheries to form DB couples. Diffusion bonding was carried out in an ABB Q1H-9 Mini HIPper using temperatures in the range 750–990 °C, pressures of 1–10 MPa and times of 1–240 min.

Specimens were prepared for metallographic examination (either un-etched or etched) using standard polishing techniques, with the polished surface being perpendicular to either the rolling or grinding direction. Etching was carried out using a reagent comprising $2HF–10HNO_3–88H_2O$ (vol %) for titanium alloys, and electro-etching, using 10 g potassium hydroxide plus 100 ml water and 5 volts, for the stainless steel.

To measure the mechanical strength of the diffusion bonds, lap shear test pieces were machined from the bonded couples with the overlap being perpendicular or parallel to the rolling or grinding direction. The specimens which had an overlap length of $\sim 1.5\,t$, where t is the thickness, were tested under compressive load with constraining to minimize bending.

3. Defects in diffusion bonds

There are various ways to obtain diffusion bonds experimentally, and the most useful technique is to HIP (hot isostatic press) EB (electron beam) welded couples as described earlier. Alternatively, specimens can be made into blocks or bars and bonded in uniaxial compression or sheet materials can be bonded in a platen press where the bonding essentially occurs in plane strain [5, 6].

One major difference between conventional fusion welds and solid phase DB welds is the defect size in incomplete bonds. In fusion welds, defects are usually formed by hot tearing or incomplete weld penetration.

TABLE I Shear strengths of bonds produced in a microduplex stainless steel at pressure of 2.1 MPa (the shear strength of parent material is $\approx 510\ MNm^{-2}$) [14]

Surface finish	Bonding temp. (K)	Bonding time (h)	Shear strength (MNm^{-2})
As-received	1280	2	311
		4	458
	1320	2	352
		6	486
Polished	1280	2	331
		4	494
	1320	2	502
		4	480

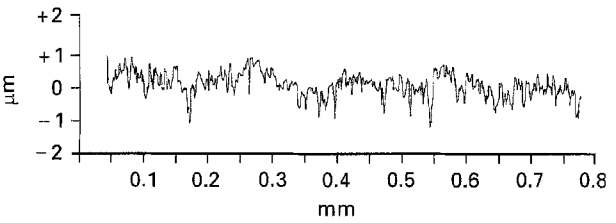

Figure 1 Surface roughness traces for an as-rolled microduplex stainless steel, showing two-wavelength feature such that a short-wavelength ($\lambda = 16\ \mu m$, $R_a = 0.2\ \mu m$) is imposed on a long-wavelength ($\lambda = 530\ \mu m$, $R_a = 0.5\ \mu m$).

The resulting defects are often large in size (on the scale of millimetres), although few in number. In diffusion bonding and other solid-phase bonding techniques, the size of defects is determined principally by the scale of roughness of the surfaces being bonded. The difference in scale of defects is so great that the techniques developed for flaw assessment in fusion welds are not sensitive enough to detect the much smaller defects in diffusion bonds [9, 12].

The surface roughness is dependent on the material and manufacturing technique. For sheet materials, the as-received surface roughness is determined by the rolling process. Previous experimental results and modelling studies show that the finer the roughness of the surface prior to bonding, the more rapid the bonding will be [2, 3, 13, 14]. Table I shows the shear strengths of bonds produced in a microduplex stainless steel for an as-rolled surface finish and a polished (finer) surface finish. It is seen that the shear strength increases more rapidly for the polished surface finish than for the as-rolled surface finish for given bonding temperatures and pressures [14]. In commercial DB practice, very fine scale roughnesses are expected to give corresponding small defect sizes in the interface.

The as-rolled surface finish often shows a bimodal distribution of asperities, which means that short-wavelength asperities are superimposed on long-wavelength asperities. Fig. 1 shows a two-wavelength feature of an as-rolled surface finish for a microduplex material as measured by a Talysurf. In diffusion bonding, the mechanism of bond formation is believed to involve instantaneous plastic collapse of the points of contact giving localized intimate metal-metal contact. The two surfaces are usually brought together with their grinding or rolling marks parallel so creating long, cylindrical voids of a maximum cross-section

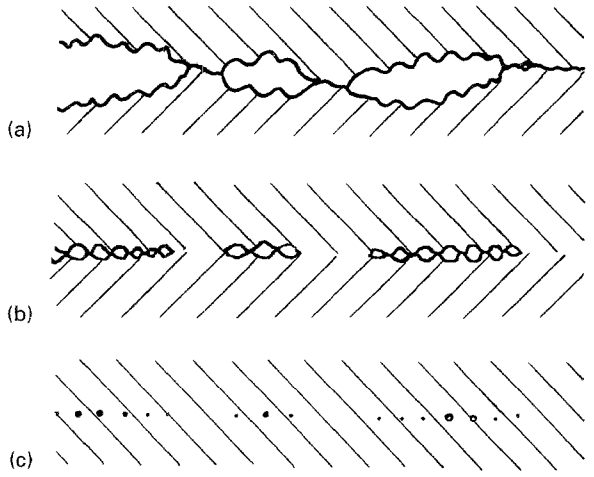

Figure 2 Schematic of development of interfacial voids from surface roughness at (a) initial, (b) intermediate and (c) later stages of bonding.

determined by the initial roughness, as schematically illustrated in Fig. 2. This is followed by removal of interfacial voids through diffusional and creep processes [2, 3].

Recently, Lutfullin *et al.* [4] and Kaibyshev *et al.* [5] have proposed that superplastic deformation i.e., grain boundary sliding and grain rotation, is the dominant mechanism of interfacial void closure and they suggested that the process should be termed as 'solid state joining' (SSJ) instead of diffusion bonding (DB). However, the spherical voids and rounded neck regions observed in the present work for titanium alloys suggest that diffusion processes play an important role when interfacial voids are very small. This occurs in the later stages of bonding, or in the bonding of surfaces with fine surface finishes, as predicted by theoretical models [2, 3], within the pressure range of the present experimental work.

4. Evaluation of diffusion bonds

4.1. Metallographic methods

4.1.1. *Light microscopy and scanning electron microscopy (SEM)*

For convenience the three bond conditions, i.e., fully bonded, partially bonded and weakly bonded specimens, examined in this section are coded as, F, P and W, respectively. Fig. 3 shows light micrographs of three IMI834 specimens bonded as above. It is seen that in the fully bonded specimen F (Fig. 3a), there is very little sign of a bond line and the interface could only be identified with the assistance of EB weld marks at the edges of the bond. In the weakly bonded specimen W (Fig. 3c), an almost continuous bond line can be seen, while, specimen P (Fig. 3b) lies between the two extremes. For the titanium alloys investigated, the incomplete bond line can be easily identified even in the very late stages of bonding by the presence of a few isolated voids [15]. This is because void dimensions in the direction perpendicular to the bond interface remain large enough for metallographical detection, presumably because surface diffusion maintains the sphericity of the neck regions of the voids

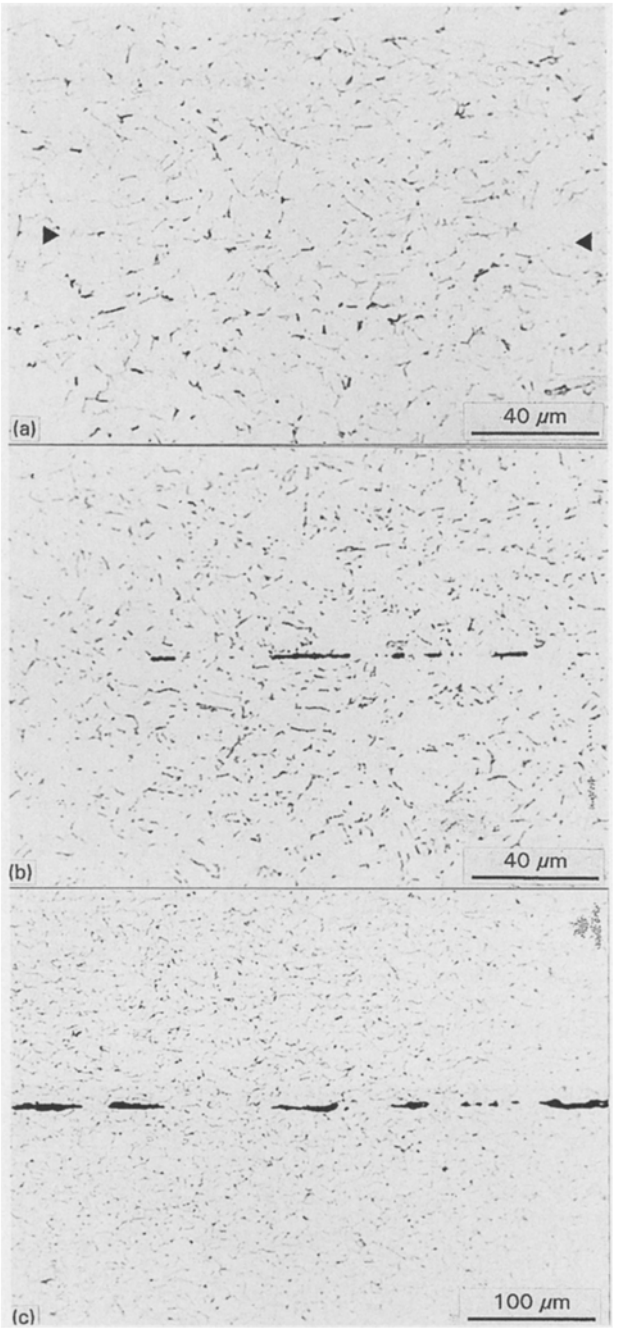

Figure 3 Light micrographs showing IMI834 bonded to various extents: (a) fully bonded specimen F, (b) partially bonded specimen P and (c) weakly bonded specimen W; arrows indicate bond line.

[3, 12]. For this type of void, not only qualitative but also quantitative assessment of area fraction bonded may be obtained using light microscopy techniques, e.g. image analysis systems, because well defined voids are present.

However, for the stainless steel specimens, void dimensions in the direction perpendicular to the bond interface are small even for the weakly bonded specimens, possibly because surface contamination prevents the operation of surface diffusion. In this case, reliable quantitative information is difficult to obtain even at the highest magnifications ($\sim 1000\times$) for light microscopy, because there is often no clear border between bonded and unbonded regions, as is seen in Fig. 4. For observations at this high magnification, special care should be taken in preparing specimens in

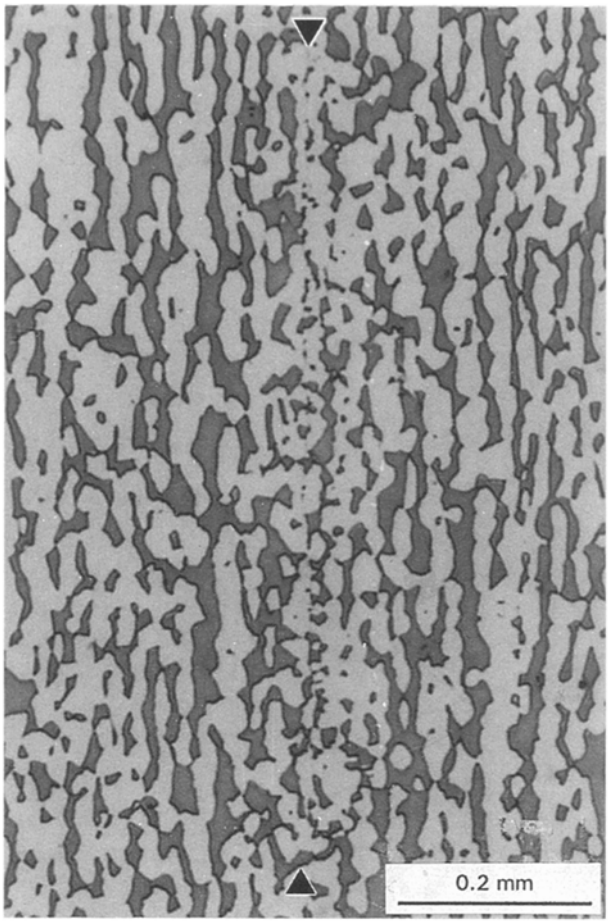

Figure 4 Light micrograph showing a weakly bonded stainless steel specimen. Although interfacial voids could not be resolved (compare with Fig. 3 (b and c)), the specimen showed zero strength; arrows indicate bond line.

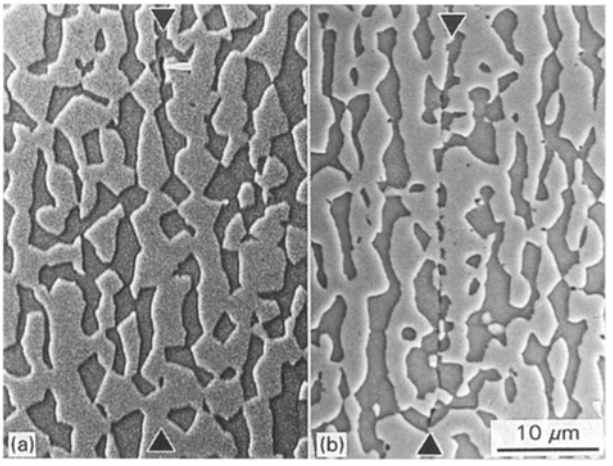

Figure 5 SEM micrographs, (a) a "fully bonded" specimen and (b) the same specimen as shown in Fig. 4; arrows indicate bond line.

order to produce flat and well polished smooth surfaces for observation. Another drawback of light microscopy is that both voids and oxides will appear as black spots or stringers, which sometimes makes it difficult to distinguish between the two features.

SEM has proven to be a useful technique to examine narrow interfacial defects such as those shown in Fig. 4. The improved resolution and much higher magnifications of SEM reveal gaps in the bond interface, Fig. 5b. Very small defects which may exist (Fig. 5a) can also be identified using SEM, while such defects often cannot be seen using light microscopy. However, the bond line may not be easily located by using SEM as compared with light microscopy, particularly for higher bonded area fractions, because large areas need to be scanned.

By observing the shape of residual voids in the bond interface, bonding mechanisms can be postulated [12]. Sharp corners in the neck regions reflect plastic collapse, whilst spherical voids indicate that diffusion from surface sources is operating.

4.1.2. Scanning acoustic microscopy (SAM)

The images in SAM are obtained by using an ultrasonic beam. However, this technique is different from the more conventional ultrasonic testing used for the assessment of fusion welds, for example, in the conventional ultrasonic technique, ultrasonic vibrations are transmitted through the material being tested. When these vibrations intersect a discontinuity, e.g., a void, they are reflected and so the discontinuity is detected. The basic requirement for this type of technique is that the dimensions of the defects should be greater than the wavelength of the signal. Unfortunately, the ultrasonic vibrations used have a frequency in the range of tens of MHz. Since the speed of sound in metals is typically about 5000 ms^{-1}, this gives a wavelength in the range of about 100–200 μm. This wavelength is considerably larger than the defects expected in the later stages of diffusion bonding and so the defects would not be detected [9, 16].

In SAM, the ultrasonic beam (which is usually of a much shorter wavelength than used for conventional ultrasonic inspection) is focused to a spot whose size is limited chiefly by diffraction to about one wavelength, and a scanned image is then built up. Diffusion bonds formed between two pieces of a medium carbon steel (En8) have previously been examined in an SAM operating at 140 MHz [9]. At this frequency, the resolution was not good enough to produce clear images of the defects in the bond line. With the improvement of SAM technology, much higher frequencies can now be produced and hence much better resolution can be obtained. By adjusting the displacement of the specimen surface relative to the focal plane of the lens (defocus), accumulated information for a certain depth (usually tens of microns) beneath the surface can be obtained.

The SAM images taken at 550 MHz for stainless steel specimens bonded to various extents are shown in Fig. 6. In the fully bonded specimen F (Fig. 6a), no sign of the bond line can be seen. In the weakly bonded specimen W (Fig. 6c), a clear continuous bond line is observed. For the partially bonded specimen P (Fig. 6b), discontinuous signs of the bond line are apparent. These images were obtained in a defocus of $z = -6$ μm (where z is the displacement of the specimen surface relative to the focal plane of the lens, forward lens is negative), which shows the accumulated information of the bond interface for a distance of 6 μm beneath the surface. The images for the same area in specimen P were obtained in defocus ($z = -8$ μm) and focus ($z = 0$ μm), and are shown in Fig. 7(a

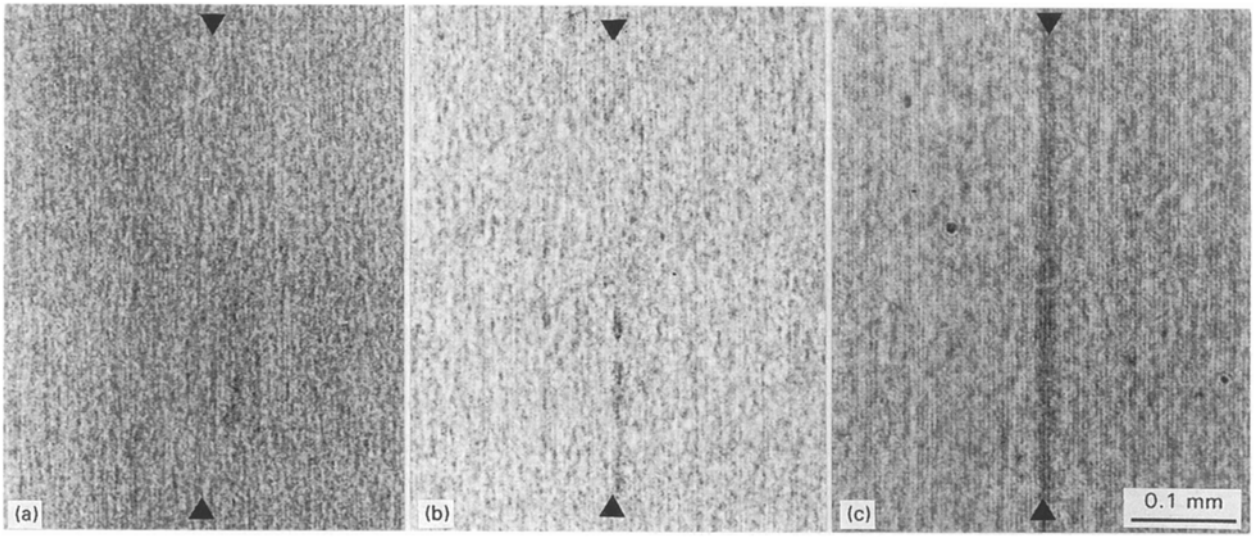

Figure 6 SAM images taken at 550MHz and $z = -6$ μm for stainless steel specimens, showing (a) fully bonded specimen F, (b) partially bonded specimen P and (c) weakly bonded specimen W; arrows indicate bond line.

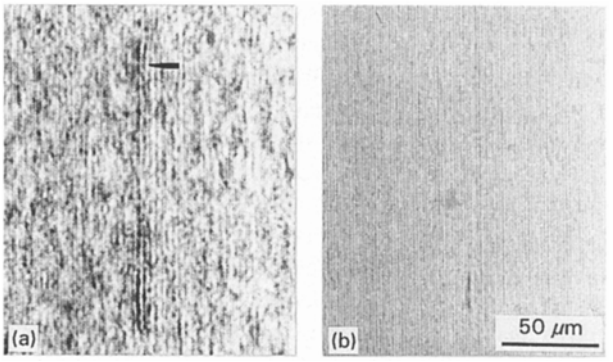

Figure 7 SAM images taken at 550MHz for the same area as in specimen P (Fig. 6b), (a) at defocus of $z = -8$ μm and (b) at focus ($z = 0$), demonstrating that defects (arrowed) in the subsurface may be detected.

and b), respectively. It is obvious, by comparing the two micrographs, that the arrowed defect in Fig. 7a is in the subsurface.

4.2. Lap shear test plus SEM observations of the fracture surfaces

The shear strengths of specimens F, P and W for IMI834 obtained under compressive load are given in Fig. 8, together with that for the parent material. It is seen that the strengths of specimens F, P and W are, respectively, about 97%, 54% and 23% of that for the parent material. These values are qualitatively in agreement with the metallographic observations using light, SEM and SAM techniques. It was also observed that the scatter of shear strength values generally increases with decreasing bond quality, as is shown in Fig. 9. It is not known if the scatter is due to some mechanical effect, such as constraint, or if it is inherent in the bonding processing, because only three specimens were used for each bonding condition. However, the void size and void distribution varies greatly at lower bonded area fractions, while, for higher bonded area fractions, and hence higher strengths, more uniformly

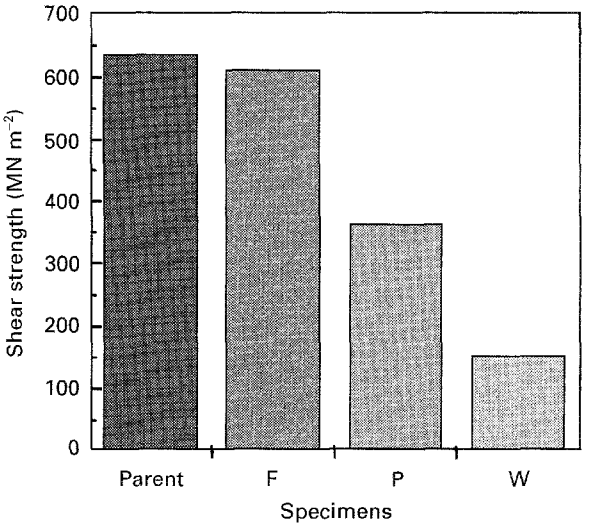

Figure 8 Shear strengths for IMI834 specimens bonded to various extents compared with parent material. F is the fully bonded, P is the partially bonded and W is the weakly bonded specimen.

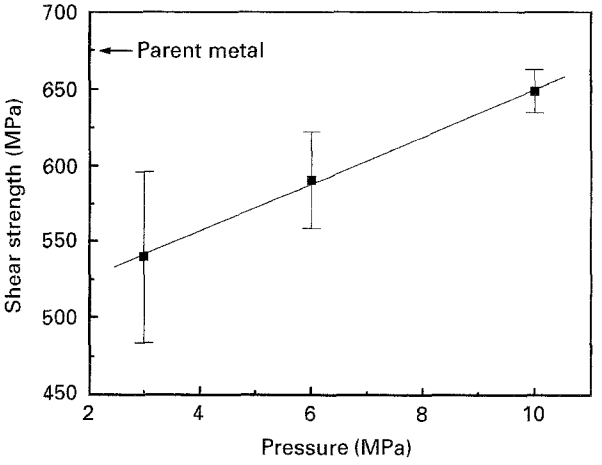

Figure 9 Effect of pressure on bond strength of IMI834 (P1200 surface finish) at 940 °C, 1 h, showing that scatter of shear strength values increases with decreasing bond quality.

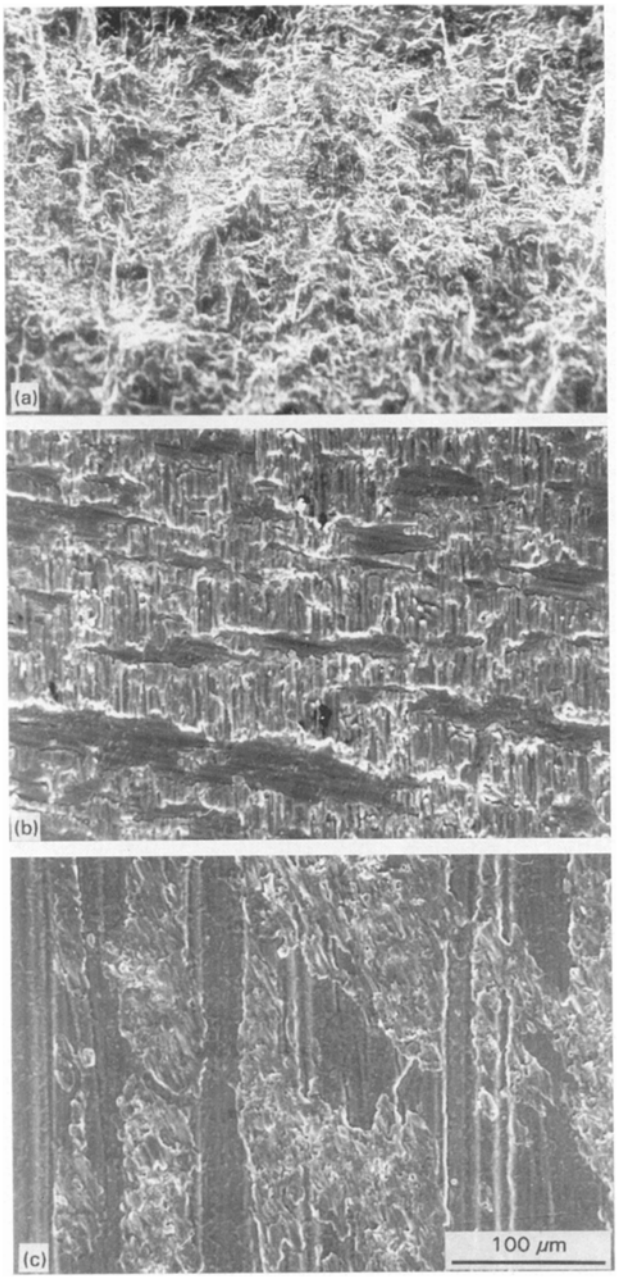

Figure 10 SEM images of the lap shear fracture surfaces corresponding to (a) specimen F, (b) specimen P and (c) specimen W in Fig. 8, showing bonded area fraction (uneven parts).

distributed spherical voids or void-free interfaces are generally observed. In view of the small overlap area used, any variation in void distribution will certainly contribute to the scatter of strength for the poor bonds.

Lap shear testing is often combined with SEM observations of the resulting fracture surfaces. Fig. 10 shows the SEM images of fracture surfaces for IMI834 specimens with bonded qualities corresponding to F, P and W. The fracture surface of fully bonded specimens, or the bonded regions of partially or weakly bonded specimens, is featured by ductile cusps as seen at a higher magnification in Fig. 11. The unbonded regions are much smoother than those shown in Fig. 11. It is seen that the bonded fractions, as indicated by the rough areas, are qualitatively in agreement with the strength for each specimen as shown in Fig. 8.

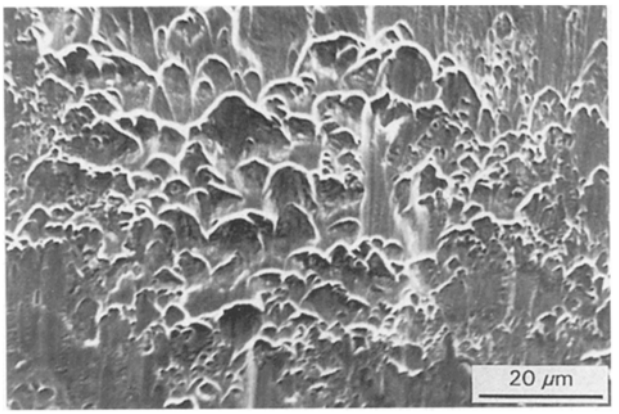

Figure 11 Same as Fig. 10a, but at a higher magnification.

5. General discussion

5.1. Relationships between metallographic observations and mechanical testing

It has been argued that bond strength, either tensile or shear, may not reflect bond quality [7, 10]. For the lap shear test used in the present work, machining of the specimens, radii at the corners, misalignment and, particularly, the constraint during testing will undoubtedly affect the measurements. However, it has been shown [6] that the shear strengths (τ) obtained under compression, with constraint, and tensile strength (σ) are consistent with the relationship of $\tau \sim 0.6\sigma$. The present work for titanium alloys also shows that the ratio of the observed bond strength to parent metal strength (referred to as percentage strength) has a linear relationship with the bonded area percentage, as obtained metallographically using an image analysis system (Magiscan), as is seen in Fig. 12.

Fig. 12 also includes the theoretical line of slope = 1, and it can be seen that the percentage strength is 5–10% lower than expected, with greater discrepancies being observed for the poor bond qualities. This may arise from two reasons: (i) stress concentrations caused by the defects and (ii) the apparent continuity of grains across a bond line is not necessarily a sufficient criterion of good bond.

These observations are significantly different from previous work on a mild steel [10] and Ti–6Al–4V [11], which showed that parent metal tensile strength could be achieved when bonded area fractions were higher than ~80%. In the present work on titanium alloys with bond shear strengths near that of the parent metal, no un-bonded regions were observed by light microscopy, by SEM of metallographic specimens or of specimens fractured during shear testing. In contrast, for metallographically sound (~100%) bonds, shear strengths as low as 85% of that of the parent metal were sometimes obtained, Fig. 12. The reason for this difference is not clear. However, in previous work on mild steel or Ti–6Al–4V [10, 11], bonding was carried out using uniaxial loading.

The percentage shear strengths in the present work for IMI834 were calculated using the shear strength of as-received material (675MPa for IMI834), which may under estimate the percentage strength. However, the uncertainty is within 4%, because the maximum bond

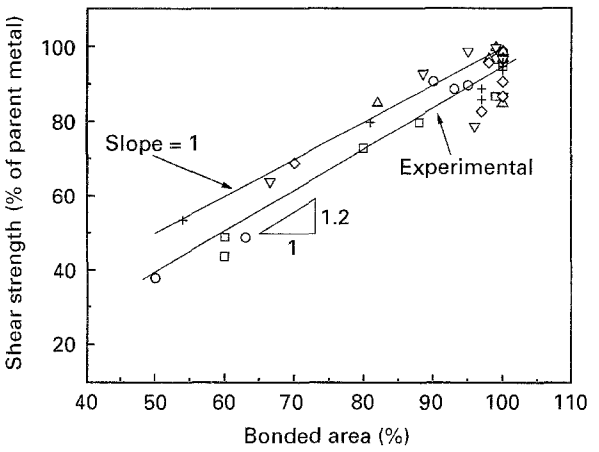

Figure 12 Relationship between percentage of parent shear strength and bonded area percent for the titanium alloys (□) IMI834/IMI834, (○) IMI834/Ti-64, (△) SP700/SP700, (▽) SP700/Ti-64, (◇) Ti-6242/Ti-6242 and (+) Ti-6242/Ti-64.

strength obtained was 650MPa. If the parent metal had undergone the same thermal cycle as the bonded specimen, its shear strength would be expected to be within the range 650–675MPa. For SP700 and Ti–6–2–4–2, the percentage shear strengths were calculated using the measured shear strengths of the parent metals, which had undergone the same thermal cycle as the bonded specimen. Results showed that the thermal treatment experienced during diffusion bonding did not significantly affect the shear strength of the materials. The shear strength of as-received SP700 materials was 625MPa, while the lowest strength for parent specimens which had undergone the thermal cycle was 590MPa.

5.2. Potential of non-destructive testing

Non-destructive evaluation of DB bonds using ultrasonic inspection [11, 16] and electric resistivity measurement [9] have been previously reported. As mentioned earlier, the conventional ultrasonic technique is unsuitable for the detection of fine defects in DB bonds.

The electrical conductivity of a piece of metal is proportional to the area through which electrons can migrate. If there is a partial bond in the material this migrational area will be reduced in the region of the bond and thus the resistance of the material will be greater than that of a similarly sized perfect specimen. The standard technique for measuring the resistance of such a bond is the four point contact method, in which a large constant current is passed along the specimen between two power contacts and the potential difference between two other contacts on the specimen surface is measured. The voltage drop along a length of specimen containing the bond can be compared with that of an identical length of perfect material and there should be a simple relationship between the difference in conductivity and the total bonded area. Based on those considerations, an attempt has been made previously to verify nominally good diffusion bonds with equipment normally used for crack propagation monitoring in fatigue experiments [9]. A problem with the technique is that the changes being observed are so small that they may be swamped by minute variations in experimental conditions or material properties. Nevertheless some workers have reported a certain amount of success using the technique [17]. However this was only for the very early stages of bonding when the actual bonded area was very small and the potential difference correspondingly large.

A further non-destructive technique is inspection by laser-generated ultrasound. The most attractive features of this technique is that it is used remote from the specimen and can be used at high temperatures, which may provide the ability of *in situ* monitoring of the bonding process. This technique has been successfully applied to the inspection of the quality of adhesive bonds, defects in composites and fatigue cracks [18–20]. However, as the frequency of the ultrasound is about 20 MHz, only defects of size ~250 μm can be detected, which makes it unsuitable for the inspection of diffusion bonds.

6. Conclusions

Light and SEM metallographic observations are the most convenient and reliable methods for qualitative assessment of the bond quality, and in the case of titanium alloys it is possible to obtain quantitative data on the extent of bonding. High frequency ultrasonic scanning acoustic microscopy also proved to be an effective procedure. With this technique, not only the defects in the surface, but also those in a few microns beneath the surface may be observed, which provides accumulated information about bond quality. A linear relationship between fraction of parent metal strength achieved and bonded area fraction as determined by metallography was observed for titanium alloys.

Acknowledgements

The authors would like to thank EPSRC for the award of an ROPA Research Grant, Dr Z. X. Guo, Queen Mary and Westfield College and Dr Q. Shan UMIST, for helpful discussions and Dr J. Pilling, Michigan Technological University, USA, for analysing the Talysurf traces.

References

1. M. S. YEH and T. H. CHUANG, *Scripta Metall. Mater.* **33** (1995) 1277.
2. J. PILLING, *Mater. Sci. Engng* **100** (1988) 137.
3. A. HILL and E. R. WALLACH, *Acta Metall.* **9** (1989) 2425.
4. Y. YA. LUTFULLIN, R. M. IMAYEV, O. A. KAIBYSHEV, F. N. HISMATULLIN and V. M. IMAYEV, *Acta Metall. Mater.* **33** (1995) 1445.
5. O. A. KAIBYSHEV, R. YA. LUTFULLIN and V. K. BERDIN, *ibid* **42** (1994) 2609.
6. A. WISBEY and P. G. PARTRIDGE, *Mater. Sci. Tech.* **9** (1993) 441.
7. D. V. DUNFORD and P. G. PARTRIDGE, in "Diffusion Bonding", edited by R. Pearce, (SIS, Cranfield, 1987) p. 17.
8. J. L. TURNER, *ibid*, p. 203.
9. B. DERBY, G. A. D. BRIGGS and E. R. WALLACH, *J. Mater. Sci.* **18** (1983) 2345.

10. S. ELLIOT, A. BUCKLOW and E. R. WALLACH, *ibid* **15** (1980) 2823.
11. M. OHSUMI, S. KIYOTOU and M. SAKAMOTO, *Trans. ISIJ* **25** (1985) 513.
12. B. DERBY and E. R. WALLACH, *Met. Sci.* **16,** (1982) 49.
13. G. GARMONG, N. E. PATON and A. S. ARGON, *Metall. Trans.* **6A** (1975) 1269.
14. N. RIDLEY, M. T. SALEHI and J. PILLING, *Mater. Sci. Tech.* **8** (1992) 791.
15. N. RIDLEY, Z. C. WANG and G. W. LORIMER, in Proc. 8th Int. Conf. Titanium. Birmingham, 1995.
16. S. E. USHAKOVA, E. S. VOLKOV and V. I. KOVRICIN, *Svarka Proiz.* **14** (1967) 29.
17. T. ENJYO, K. IKEUCHI and N. AKIKAWA, *Trans. Jpn. Welding Research Inst.* **7** (1978) 97.
18. R. INCE, G. E. THOMPSON and R. J. DEWHURST, *J. Adhesion* **42** (1993) 135.
19. Q. SHAN and R. J. DEWHURST, *Appl. Phys. Lett.* **62** (1993) 2649.
20. R. J. DEWHURST, R. HE and Q. SHAN, *Mater. Evaluation* (1993) 935.

Received 6 March
and accepted 24 May 1995